Submitted to ADVANCED OPTICAL MATERIALS

DOI: 10.1002/adom. ((please add manuscript number))
Article type: Communication

1,7-Bay-Substituted Perylenediimide derivative with Outstanding Laser Performance

Manuel G. Ramírez, Sara Pla, Pedro G. Boj, José M. Villalvilla, José A. Quintana, María A. Díaz-García Fernando Fernández-Lázaro and Ángela Sastre-Santos**

Dr. M.G. Ramírez, Prof. J.M. Villalvilla and Prof. M.A. Díaz-García
Dpto. Física Aplicada, Instituto Universitario de Materiales de Alicante and Unidad Asociada UA-CSIC; Universidad de Alicante, Alicante 03080, Spain
E-mail: maria.diaz@ua.es

Prof. P.G. Boj and Dr. J.A. Quintana
Dpto. Óptica, Instituto Universitario de Materiales de Alicante and Unidad Asociada UA-CSIC; Universidad de Alicante, Alicante 03080, Spain

S. Pla, Prof. F. Fernandez-Lázaro and Prof. Á. Sastre-Santos
División de Química Orgánica Instituto de Bioingeniería, Universidad Miguel Hernández, Elche 03202, Spain.
E-mail: asastre@umh.es

Keywords: amplified spontaneous emission; laser; perylenediimides; bay-substituted

Dye lasers have been widely employed in spectroscopy, photochemistry, photophysics, nondestructive testing and medicine,[1] being the most interesting property the capability of tuning the emission wavelength within the visible range. However, their use has been certainly limited by the need to disperse the dye in a liquid solution in order to prevent photodegradation as well as photoluminescence (PL) quenching due to molecular interaction. In the last years, many efforts have been devoted to the development of compact and easy-to-handle solid-state organic lasers based on active materials of various kinds: dye-doped inert polymers (typically thermoplastics), semiconducting materials (polymers, oligomers, dendrimers or small molecules) and single crystals.[1] Many studies have focused in decreasing the pump intensity needed to achieve laser emission (i.e. the threshold), aiming to reduce pumping requirements. Another aspect of interest, particularly challenging in the case of single crystals,[1d] consists in fabricating flexible devices, and thus exploiting one of the main advantages or organics versus inorganics. At this respect, dye-doped polymers offer

many possibilities, thanks to the technologies available to process thermoplastics. Finally, a property that has generally received less attention, despite its huge importance from a practical point of view is the photostability. This is one of the key advantages of dye-doped polymers with respect to other materials, mainly because the dilution of the dye in a matrix. In the context of laser dyes, there is still room for improvement. Thus for example, commercial long-wavelength fluorescent dyes have a number of applications, but display severe limitations like poor photostability and chemical stability and/or low absorption at the standard pump wavelength.[2]

Perylenediimides (PDIs) are chemically very resistant organic molecules displaying a substituent-dependent huge absorption in the 450-600 nm region, bright fluorescence with quantum yields close to unit and high thermal and chemical stability, as well as photostability.[3] Moreover, a great variety of PDI derivatives are synthetically accessible by introduction of the adequate substituents, thus allowing tailoring their optical and red-ox properties.[3,4] All these characteristics, together with several others such as their high electron affinity and mobility, transform PDIs into valuable pieces for the fabrication of a wide variety of optoelectronics and biological applications.[5] Among them, the one of interest in this work is the optically-pumped laser.

Distributed feedback (DFB) lasers based on optically inert polymer films [e.g. polystyrene, PS, or poly(methyl methacrylate), PMMA] doped with PDIs have been recently reported.[6-8] In DFB lasers, feedback is achieved by modulating either the refractive index or the gain of the active medium,[1] for example by recording a grating in the substrate[6,7] or in the active film.[8] PDI-based DFB lasers have shown operational lifetimes (under ambient conditions) among the highest reported, [6a] while keeping reasonable thresholds. Typical PDI concentrations in the polymer matrix are quite low, i.e. ~ $(0.5\text{-}1)\times10^{-5}$ mol of PDI per gram of PS (equivalent to 0.5-1 wt% of PDI with respect to PS), since higher values generally lead to

PL quenching and therefore to a reduced performance.[6d,9] This establishes limitations in the laser efficiency and threshold, generally lower than those of non-diluted active materials, such as semiconducting PL polymers.[1] At this respect, a challenge to reduce the thresholds of PDI-based lasers would be to increase the PDI content in the films.[9a] On the other hand, dispersing the active laser material in a matrix improves the photostability considerably. Indeed, this property is generally superior in dye-doped polymers than in other materials, such as single crystals or semiconducting polymers,[6a,1] although in fact for these latter materials there are just a few studies on this issue.[1] At this respect, certain PDIs are among the materials with the highest laser photostabilities reported.[6a,6d,9a] Another attractive property of PDI-doped PS films is that their thermal and optical properties keep unaltered after being heated up to temperatures of around 155 ºC. This has allowed engraving high quality DFB structures directly on the active materials,[8] by using thermal nanoimprint lithography (NIL). This technique, which has a great potential to be scaled to volume production, cannot generally been used to imprint organic semiconductors, since their optical properties are degraded by the high temperatures.[1]

Up to now, all reported perylenediimide-based lasers are made of PDIs without substituents at the bay positions (denoted here as *u*-PDIs, with "*u*" accounting for *bay*-unsubstituted),[6-8] as a consequence of previous studies on the amplified spontaneous emission (ASE) properties of waveguides containing perylene derivatives with different chemical structures (e.g. imide, anhydride), which concluded that *u*-PDIs had the best performance.[9] It is known that ASE characterization is the simplest and most convenient method to asses the potential of a given material for laser applications based on active waveguide films.[1,9] ASE is evidenced by the observation, at a certain optical pump intensity, of a collapse of the width of the PL spectrum and a large enhancement of the output intensity, thus indicating the presence of gain due to stimulated emission. In a previous work, we

compared the ASE performance of *u*-PDI-doped PS to that of other materials such as pyrromethenes dispersed in PMMA and to various semiconducting oligomers and polymers.[9a] The photostabilities of *u*-PDIs are among the highest reported. Their thresholds are significantly lower than those of other highly photostable dye-doped systems, and larger than those of non-diluted molecular materials or semiconducting polymers (by typically one order of magnitude). Nevertheless, the photostability for these latter systems is very limited.

u-PDIs are characterized by absorption and PL spectra practically independent on the type of substituent attached to the *N* atoms because of the nodes of the HOMO and LUMO at the imide nitrogen's.[3] So, when doped into a polymer film, irrespective of the particular *u*-PDI derivative, ASE appears at the same wavelength (around 579 nm).[6d,9] In addition, this value can not be shifted to longer wavelengths by increasing the dye concentration in the matrix, as can be done with other materials,[10] since the range of *u*-PDI concentrations which provide ASE is very limited.[6d,9b,9f] Therefore, designing PDIs emitting at longer wavelengths and showing good laser characteristics is of great interest. This was precisely the motivation in previous works devoted to the ASE investigation of *bay*-substituted PDIs (denoted as *b*-PDIs, with "*b*" accounting for substitutions at bay positions in the core).[9a,9c-9e] Unfortunately, their ASE performance was rather poor, mainly due to their low PL quantum yield, as a result of their distorted PDI core.[9a,c] For this reason, up to now, *b*-PDIs have not been used to fabricate laser devices. In this context, during the progress of this work some authors have synthesized a *b*-PDI derivative, particularly a 1,7-bis(diphenylphenoxy)PDI, with an undistorted core and, thus, a PL quantum yield in solution close to unity.[11] In addition, thanks to the bulky groups attached, high PL quantum yields (37%) were obtained in solid state (single crystals).

In this communication, efficient ASE emission at wavelengths between 610 and 630 nm, from PS films doped with a highly solid state fluorescent PDI derivative (denoted as *b*-

PDI-1) is demonstrated. *b*-PDI-1 is a bay-substituted PDI presenting two sterically hindering diphenylphenoxy groups at the 1,7 position and ethylpropyl substituents in the imide positions [see chemical structure in Figure 1(a)]. ASE has been observed for a very wide range of *b*-PDI-1 concentrations and up to values as large as 37 $\times 10^{-5}$ mol of PDI per gram of PS (*i.e.* 27 wt% of PDI with respect to PS). This is much higher (around 40 times) than typical PDI concentrations used in prior laser studies. Thanks to this significant increase in the PDI content in the film, very high PL and ASE efficiencies, as well as low ASE thresholds, have been obtained. A detailed investigation of the various ASE parameters, including photostability, has allowed establishing criteria to design optimized devices based on these materials for a given application. Finally, a DFB laser device using one of the best performing films has been fabricated and characterized.

The synthetic procedure of *b*-PDI-1 is described in the supporting information. The absorption (abs) and PL spectra of *b*-PDI-1 in $CHCl_3$ solution show the typical vibronic structure of PDIs,[3,9a] with maxima at λ_{max}^{abs} = 563 nm (for abs) and at λ_{max}^{PL} = 579 nm (for PL) (see SI, Fig. S1). The molar extinction coefficient (ε) was 69700 (at λ_{max}^{abs}) and 30240 (at the pump wavelength used for ASE and laser characterization, λ_{pump} = 532 nm). The measured PL quantum yield (ϕ_{PL}) in $CHCl_3$ was the unity, indicating an undistorted core, in agreement with results obtained previously with a similar derivative.[11] This ϕ_{PL} value is much larger than that of most *b*-PDIs reported in the literature.[9a]

The shape and relative intensity of the bands in the abs and PL spectra for the *b*-PDI-1-doped PS films [see SI, Fig. S2 and Fig. 1(c)] are very similar to those obtained in solution, for any doping ratio within the investigated range. This is in contrast with the behaviour of other PDIs, whose film spectra change considerably as a function of the PDI content, effect generally attributed to the formation of aggregated species.[6d,9a] The capacity of introducing large amounts of *b*-PDI-1 in the films, without getting significant PL quenching, is illustrated

in Figure 1(b). As observed, PL intensity increases almost linearly with the *b*-PDI-1 content, up to around 37×10^{-5} mol of PDI per gram of PS (the preparation of films with larger concentrations was limited by solubility). This increase in PL is a direct consequence of the increase in film absorption: the absorption coefficient at λ_{pump} varied linearly from 1.3×10^3 to 4.5×10^4 cm^{-1}, for the same range of PDI concentrations (see SI, Fig. S3). The stimulated emission cross section at λ_{ASE} [$\sigma_{em}(\lambda_{ASE})$] and the absolute PL quantum yield (PLQY) were determined for all the films following methods previously described (more details in SI, experimental).[12] Values varied from 5×10^{-17} to 2×10^{-17} cm^2, for $\sigma_{em}(\lambda_{ASE})$, and from 76 to 32%, for PLQY (see inset of Fig. 1(b)). Both parameters have a similar type of dependence: they decay as the concentration increases, but not significantly. So, although this is indicative of the existence of intermolecular interaction, the effect is small, thus justifying the fact that the shape of the absorption and PL spectra keep practically unaltered. An important point is that even for the films with the highest concentration, a PLQY value as large as 31% was obtained. In order to highlight the unique properties of *b*-PDI-1, results for two other PDI derivatives (denoted as *u*-PDI-2 and *b*-PDI-3, see chemical structure in Figure 1a), whose spectral and laser properties were previously studied, have been included. In particular, *u*-PDI-2 with 2,6-diisopropylphenyl groups attached to the imide positions, has been the best performing PDI laser dye, when dispersed at concentrations of (0.5-1) wt% into polymers such as PS or PMMA.[6d] On the other hand, *b*-PDI-3, with 4-*tert*-butylphenoxy groups at the 1,7-bay positions and 2-ethylhexyl substituents at the imides, showed a very poor ASE performance at any concentration, mainly due to its low PL efficiency, both in solution and in thin film.[9a] It is remarkable that the large dye doping ratios achievable with *b*-PDI-1 allow increasing film absorption and PL intensity, with respect to other PDIs previously reported (Fig. 1b) . As will be shown below, an important consequence of this will be the increase in the output ASE intensity.

ASE was observed in the *b*-PDI-1-doped films under nanosecond pulsed excitation. Films approximately 550 nm thick were optically pumped at λ_{pump} = 532 nm with a striped laser beam of dimensions 3.5 × 0.5 mm^2 and the light emitted from the end of the stripe was collected with a fiber spectrometer. Figure 1(c) shows the ASE spectra obtained for some of them, including the ones with the lowest and highest *b*-PDI-1 contents. The corresponding PL spectra have also been represented in the figure. For comparison purposes, these spectra have been normalized in order to show similar intensity, although obviously, the emitted PL and ASE intensity increase with the *b*-PDI-1 amount present in the sample. ASE appears at the most intense vibronic transition, i.e. the 0–1 transition, and not at the 0–0 component, whose intensity is much higher. It is a common situation in many materials reported in the literature and is caused by re-absorption due to the proximity between absorption and PL.[1] This is the case for all the PDI derivatives previously investigated,[6d,9] as well as for the *b*-PDI-1 compound studied here. In some materials ASE has been observed at other vibronic transitions with lower PL intensity, due to the presence of triplet absorption or photoinduced absorption in the region of the first vibronic peak.[1g] An important consequence of increasing the range of PDI content in the films, is that the ASE wavelength can be tuned over a relatively wide range (around 20 nm, from *ca* 610 to 630 nm, see Fig. 1(c)). This is a clear advantage over *u*-PDIs, for which, as previously mentioned, ASE emission appears always at around 579 nm.

The ASE intensity for various films (doped with different *b*-PDI-1 contents) has been plotted in Figure 2(a) as a function of the pump intensity. From these plots, the ASE threshold, defined as the intensity at which a clear increase of the output intensity is observed, has been determined. Besides this parameter, which is the most commonly used in the literature to quantify the ASE performance, it is also useful to analyze the output power obtained. Qualitative, this can be done by simply looking at the output intensity obtained for a given

pump intensity. For a quantitative analysis, the slope efficiency, i.e. the slope of the emission intensity curve above the threshold is often determined in the context of laser devices.[1a,1b] It should be noted that in order to obtain an absolute value of slope efficiency, all the energy emitted by the device should be collected. In fact, quantitative measurements of the output power from organic lasers are sparse in the literature.[1a,1b] In our case, we have not obtained absolute slope efficiencies, but relative values which have been useful to analyze the effect on the output intensity of changing the PDI concentration in the film.

These two parameters (threshold and slope), determined from curves shown in Fig. 2(a), have been represented in the inset of Fig 2(a) as a function of the *b*-PDI-1 content, for all the films prepared. The particular concentrations whose data appear in Fig. 2(a) have been labelled with capital letters for a rapid identification of a given film. As observed, the lowest thresholds (around 7 kW/cm^2) and highest efficiencies have been obtained for concentrations between 6×10^{-5} and 13×10^{-5} mol of *b*-PDI-1 per gram of PS (films labelled with C and D). The PLQY for these films is around 60% (see inset of Fig. 1(b)). The drastic improvement in the performance with respect to film A (whose concentration is similar to the typical PDI concentrations used in previously reported PDI-based lasers) illustrates the unique properties of *b*-PDI-1. The decrease in threshold with concentration is explained by the increase in the absorption and PL emission (Fig. 1b). The reason for the saturation and slight increase above a certain concentration can be attributed to the saturation observed in the PL intensity (due to the decrease in PLQY), as well as to the increase in the waveguide losses. A similar type behaviour has been observed in *u*-PDIs[6d] and in other molecular materials dispersed in inert polymers at high concentrations.[10] The ASE performance of *b*-PDI-1 is outstanding in comparison to other *b*-PDIs,[9a,9c-9e] such as the *b*-PDI-3, with a much smaller output intensity and a threshold as large as 1500 kW/cm^2.[9a] The capability of introducing large amounts of *b*-PDI-1 in the films without getting PL quenching is also a remarkable result in the general

context of PDIs of any type (i.e. *u*-PDIs and *b*-PDIs), since it allows obtaining much larger output intensities, as shown in Fig. 1(b). With regards to the threshold, the impact of increasing the concentration has not been so significant, given that the best value achieved with *b*-PDI-1 is comparable to the best values obtained with *u*-PDIs (between 3 and 12 kW/cm^2, depending on the particular derivative).[6d] Nevertheless, there is still room for further improvement by optimizing various parameters, such as the overlap between the pump and the absorption wavelengths, or the waveguide properties of the films. Work at this respect is currently under way.

The ASE photostability was investigated by recording the temporal evolution of the ASE intensity under constant excitation at the same spot of the sample and under ambient conditions. Results for some of the films are shown in Figure 2(b). The parameter used to quantify this property, the ASE photostability half-life ($\tau_{1/2}^{ASE}$) is defined as the time (or the number of pump pulses) at which the ASE intensity decays to half of its initial value. Photostability characterization was performed by pumping the films in two different ways: (i) using pump intensities of around two times above their corresponding thresholds; and (ii) at the same pump intensity for all of them, being in all cases well above their threshold (i.e. 2500 kW/cm^2). The first way provides an estimate of the operational durability under moderate conditions.[6a] The second one allows comparing different materials, as well as determining the durability of the films under extreme pumping conditions.[6d] Results for all the films prepared in this work are displayed in the inset of Figure 2(b). As observed, whatever the excitation conditions, the lower the *b*-PDI-1 content, the longer the $\tau_{1/2}^{ASE}$ is. Therefore, there is a trade-off between photostability and threshold which should be taken into account when choosing the optimal concentration for a given application. For example, in applications where photostability is not relevant, such as in disposable sensors, the concentration that gives the lowest possible threshold will be a wise option.

Finally, a second order DFB laser device was fabricated by depositing a 1300 nm *b*-PDI-1-doped PS film (the one labelled as C in Figure 2) over a 190 nm dichromated gelatine (DCG) photoresist layer with a one-dimensional relief grating of period 391 nm and depth 50 nm (see Scheme of the geometry in Figure 3). The device was optically pumped at a wavelength of 532 nm. The beam was incident at an angle of 20º with respect to the normal to the film plane and shaped as an elliptical spot with a minor axis of 1.1 mm. The emitted light was collected in a direction perpendicular to the film surface. The successful performance of this type of DFB geometry (with the photoresist layer with the grating directly used as the substrate of the device) for *u*-PDI-based lasers has been just reported.[7] One advantage of such type of devices is that the fabrication process is simple and the obtained gratings are highly resistant to organic solvents, so they can be reused multiple times. The particular active film thickness value used in the device was chosen in order to obtain DFB emission associated to the fundamental transverse electric (TE_0) waveguide mode, helped by experimental waveguide characterization using the m-line technique[13] and modelling,[14] and at a wavelength close to the ASE wavelength (see Fig. 3), since these are the most important parameters to optimize the threshold.[6b,7,8] DFB emission was observed at 622.1 nm and the threshold, determined from the change in slope of the output versus input intensity curve (see inset in Fig. 3) was 55 kW/cm^2 (i.e. 6 μJ/pulse). The effect of the grating in reducing the threshold and in increasing the slope efficiency is illustrated by comparing with ASE data for a film of the same characteristics deposited over a DCG layer without grating, measured in the same experimental setup used to characterize the DFB device. The reason why this ASE threshold is higher than the one of Fig. 2 is because the different geometry for excitation and light collection, as described in detail in other works.[6c,15] At present, we are starting some work towards the fabrication of DFB lasers with gratings engraved by thermal-NIL directly on the active film, given that the thermal and optical properties of the material keep unaltered

when subjected to high temperatures,[16] as in the case of *u*-PDI-doped PS films.[8] The use of such resonators will hopefully allow reducing the threshold by several times,[6,8] approaching the requirements needed to pump with light emitting diodes (i.e. < 1 kW/cm^2).[15] In any case, the threshold value of the laser prepared in this work is of the same order (or even somewhat lower) than the best DFB thresholds obtained in similar devices (i.e. with gratings over a DCG layer used as substrate) based on an *u*-PDI derivative.[7] The device showed a photostability halflife of around 7 min (4200 pump pulses) under constant excitation at around 4 times above its threshold. This value is in accordance with previous ASE measurements [see Figure 2(b)]. As already discussed, this property can be significantly improved by decreasing the PDI content in the film, although this would imply a threshold increase.

In conclusion, efficient ASE emission at wavelengths between 610 and 630 nm, from PS films doped with a new bay-substituted PDI derivative (*b*-PDI-1) has been reported. ASE has been observed for a very wide range of *b*-PDI-1 concentrations and up to 37×10^{-5} mol of PDI per gram of PS. This maximum concentration is around 40 times larger than typical PDI concentrations used in prior laser studies. This capability of introducing large dye amounts in the film without PL quenching, allows obtaining very high PL and ASE efficiencies with low ASE thresholds as well as tuning the emission wavelength in a wide range. Criteria to design optimized devices for a given application, considering threshold, efficiency and photostability, are provided. A DFB laser device using one of the best performing films is demonstrated. Overall, this work widens the use of PDIs in laser applications, up to now restricted to bay-unsubstituted *u*-PDIs (all with ASE emission at around 580 nm), by including 1,7-bay bulky substituents in the PDI core.

Supporting Information ((delete if not applicable))

Supporting Information is available from the Wiley Online Library or from the author.

Acknowledgements

We thank support from the Spanish Government (MINECO), the European Community (FEDER) and the Generalitat Valenciana through MAT-2011-28167-C02, CTQ2011-26455,

PROMETEO 2012/010 and ISIC/2012/008, as well as to the University of Alicante and the University Miguel Hernández de Elche. We also acknowledge V. Esteve for technical assistance.

Received: ((will be filled in by the editorial staff))
Revised: ((will be filled in by the editorial staff))
Published online: ((will be filled in by the editorial staff))

[1] a) I. D. W. Samuel, G. A. Turnbull, *Chem. Rev.* **2007**, *107*, 1272; b) S. Chenais, S. Forget, *Polym. Int.* **2011**, *61*, 390; c) H. Mizuno, U. Haku, Y. Marutani, A. Ishizumi, H. Yanagi, F. Sasaki, S. Hotta, *Adv. Mater.* **2012**, *24*, 5744; d) H. Fang, R. Ding, S. Lu, X. Zhang, J. Feng, Q. Chen, H. Sun, *J. Mater. Chem.* **2012**, *22*, 24139; e) S. Varghese, S-J. Yoon, E.M. Calzado, S. Casado, P.G. Boj, M.A. Díaz-García, R. Resel, R. Fischer, B. Milián-Medina, R. Wannemacher, S.Young Park, J. Gierschner, *Adv. Mater.* **2012**, *24*, 6473; f) E.R. Martins, Y. Wang, A.L. Kanibolotsky, P.J. Skabara, G.A. Turnbull, I.D.W. Samuel, *Adv. Optical Mater.* **2013**, *1*, 563; g) J. Casado, V. Hernández, J.T. López Navarrete, M. Algarra, D.A. da Silva Filho, S. Yamaguchi, R. Rondão, J.S. Seixas de Melo, V. Navarro-Fuster, P.G. Boj, M.A. Díaz-García; *Adv. Optical Mater.* **2013**, *1*, 588.

[2] L. Cerdán, E. Enciso, V. Martín, J. Bañuelos, I. López-Arbeloa, A. Costela, I. García-Moreno, *Nature Photonics* **2012**, *6*, 621.

[3] a) F. Würthner, *Chem. Commun.* **2004**, 1564; b) H. Langhals, *Helv. Chim. Acta* **2005**, *88*, 1309; b) C. Huang, S. Barlow, S. R. Marder, *J. Org. Chem.* **2011**, *76*, 2386.

[4] a) A. Hermann, K. Müllen, *Chem. Lett.* **2006**, *35*, 978; b) G. Battagliarin, C. Li, V. Enkelmann, K. Müllen, *Org. Lett.* **2011**, *13*, 3012.

[5] a) C. Li, H. Wonneberger, *Adv. Mater.*, **2012**, *24*, 613; b) M. Guide, S. Pla, A. Sharenko, P. Zalar, F. Fernández-Lázaro, Á. Sastre-Santos, T.-Q. Nguyen, *Phys. Chem. Chem. Phys.*, **2013**, DOI: 10.1039/c3cp53552e; c) F. J. Céspedes-Guirao, A. B. Ropero, E. Font-Sanchis, A. Nadal, F. Fernández-Lázaro, A. Sastre-Santos, *Chem. Commun.* **2011**, *47*, 8307; d) V. M. Blas-Ferrando, J. Ortiz, L. Bouissane, K. Ohkubo, S. Fukuzumi, F. Fernández-

Lázaro, A. Sastre-Santos, *Chem. Commun.* **2012**, *48*, 6241; e) N. Gálvez, E. J. Kedracka, F. Carmona, F. J. Céspedes-Guirao, E. Font-Sanchis, F. Fernández-Lázaro, A. Sastre-Santos, J. M. Domínguez-Vera, *J. Inorg. Biochem.* **2012**, *117*, 205; f) Y. Yang, Y. Wang, Y. Xie, T. Xiong, Z. Yuan, Y. Zhang, S. Quian, Y. Xiao, *Chem. Commun.* **2011**, *47*, 10749.

[6] a) V. Navarro-Fuster, E.M. Calzado, P.G. Boj, J.A. Quintana, J.M. Villalvilla, M.A. Díaz-García, V. Trabadelo, A. Juarros, A. Retolaza and S. Merino, *Appl. Phys. Lett*. **2010,** *97*, 171104; b) V. Navarro-Fuster, I. Vragovic, E.M. Calzado, P.G. Boj, J.A. Quintana, J.M. Villalvilla, A. Retolaza, A. Juarros, D. Otaduy, S. Merino and M.A. Díaz-García, *J. Appl. Phys*. **2012**, *112*, 043104; c) E.M. Calzado, J.M. Villalvilla, P.G. Boj, J.A. Quintana, V. Navarro-Fuster, A. Retolaza, S. Merino and M.A. Díaz-García, *Appl. Phys. Lett*. **2012,** *101*, 223303; d) M. G. Ramírez, M. Morales-Vidal, V. Navarro-Fuster, P. G. Boj, J. A. Quintana, J. M. Villalvilla, A. Retolaza, S. Merino, M. A. Díaz-García, *J. Mater. Chem. C* **2013**, *1*, 1182.

[7] M. G. Ramírez, J. A. Quintana, J. M. Villalvilla, P. G. Boj, A. Retolaza, S. Merino, M. A. Díaz-García, *J. Appl. Phys.* **2013**, *114*, 033107.

[8] M. G. Ramírez, P.G. Boj, V. Navarro-Fuster, I. Vragovic, J.M. Villalvilla, I. Alonso, V. Trabadelo, S. Merino and M.A. Díaz-García, *Opt. Express* **2011**, *19*, 22443.

[9] a) E. M. Calzado, J. M. Villalvilla, P. G. Boj, J. A. Quintana, R. Gómez, J. L. Segura, M. A. Díaz-García, *J. Phys. Chem. C* **2007**, *111*, 13595; b) E. M. Calzado, J. M. Villalvilla, P. G. Boj, J. A. Quintana, R. Gómez, J. L. Segura, M. A. Díaz-García, *Appl. Opt.* **2007**, *46*, 3836; c) M. A. Díaz-García, E. M. Calzado, J. M. Villalvilla, P. G. Boj, J. A. Quintana, F. J. Céspedes-Guirao, F. Fernández-Lázaro, A. Sastre-Santos, *Synth. Met.* **2009**, *159*, 2293; d) A. Miasojedovas, K. Kazlauskas, G. Armonaite, V. Sivamurugan, S. Valiyaveettil, J. V. Grazulevicius, S. Jursenas, *Dyes Pigments* **2012**, *92*, 1285; e) L. Cerdan, A. Costela, G. Duran-Sampedro, I. García-Moreno, M. Calle, M. Juan-y-Seva, J. de Abajo, G. A. Turnbull, *J. Mater. Chem.* **2012**, *22*, 8938; f) E. M. Calzado, M. G. Ramírez, P. G. Boj, M. A. Díaz García,

Appl. Opt. **2012,** *51*, 3287**.**

[10] a) M.A. Díaz-García, E.M. Calzado, J.M. Villalvilla, P.G. Boj, J.A. Quintana, F. Giacalone, J.L. Segura, N. Martín, *J. Appl. Phys.* **2005**, *97*, 063522; b) E.M. Calzado, J.M. Villalvilla, P.G. Boj, J.A. Quintana and M.A. Díaz-García, *Org. Electron.* **2006**, *7*, 319; c) V. Navarro-Fuster, E.M. Calzado, M.G. Ramírez, P.G. Boj, J.T. Henssler, A.J. Matzger, V. Hernández, J.T.L. Navarrete, M.A. Díaz-García, *J Mater Chem.* **2009**, *19*, 6556.

[11] M.-J. Lin, A. J. Jiménez, C. Burschka, F. Würthner, *Chem. Commun.* **2012**, *48*, 12050.

[12] a) X. Liu, C. Py, Y. Tao, *Appl. Phys. Lett.* **2004**, *15*, 2727; b) A. Penzkofer, *Chem. Phys.* **2012**, *400*, 142; c) T. Van Der Boom, R. T. Hayes, Y. Zhao, P. J. Bushard, E. A. Weiss, M. R. Wasielewski, *J. Am. Chem. Soc.* **2002**, *124*, 9582.

[13] The film showed three waveguide modes with effective indexes of 1.59, 1.55 and 1.49 and corresponding Bragg wavelengths, calculated from Bragg equation as in ref. 7, of around 622, 606 and 583 nm respectively.

[14] Assuming the simple model used in ref. 7, effective indexes mentioned in ref. 12 could be assigned to propagation modes TE_0, TE_1 and TE_2 respectively.

[15] G. Tsiminis, Y. Wang, A. L. Kanibolotsky, A. R. Inigo, P. J. Skabara, I. D. W. Samuel, G. Turnbull, *Adv. Mater.* **2013,** *25*, 2826**.**

[16] Thermogravimetric and differential thermal analysis performed in powder samples of *b*-PDI-1 have shown that degradation starts at around 370 ºC. It was also verified that the PL and ASE of *b*-PDI-1-doped films were not affect by treatments at 155 ºC for 15 minutes.

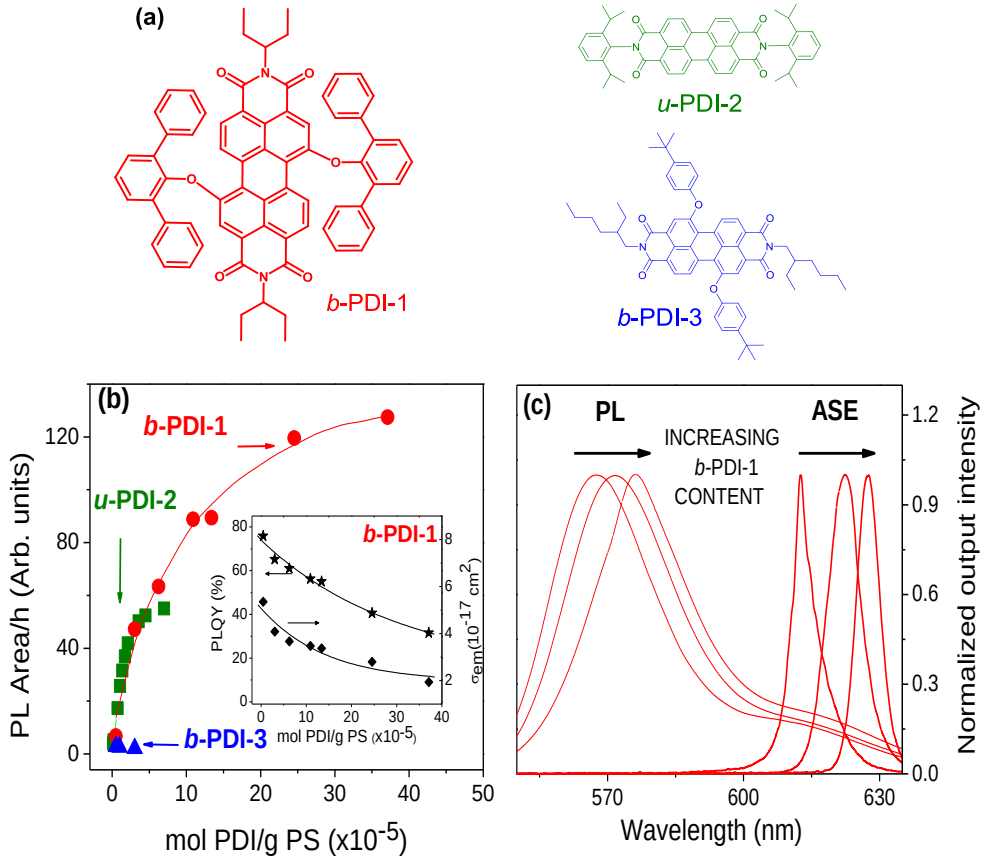
(a)
b-PDI-1
u-PDI-2
b-PDI-3
(b)
b-PDI-1
u-PDI-2
b-PDI-3
PL Area/h (Arb. units)
mol PDI/g PS (x10-5)
PLQY (%)
σem(10-17 cm2)
(c)
PL
ASE
INCREASING
b-PDI-1
CONTENT
Normalized output intensity
Wavelength (nm)

Fig. 1

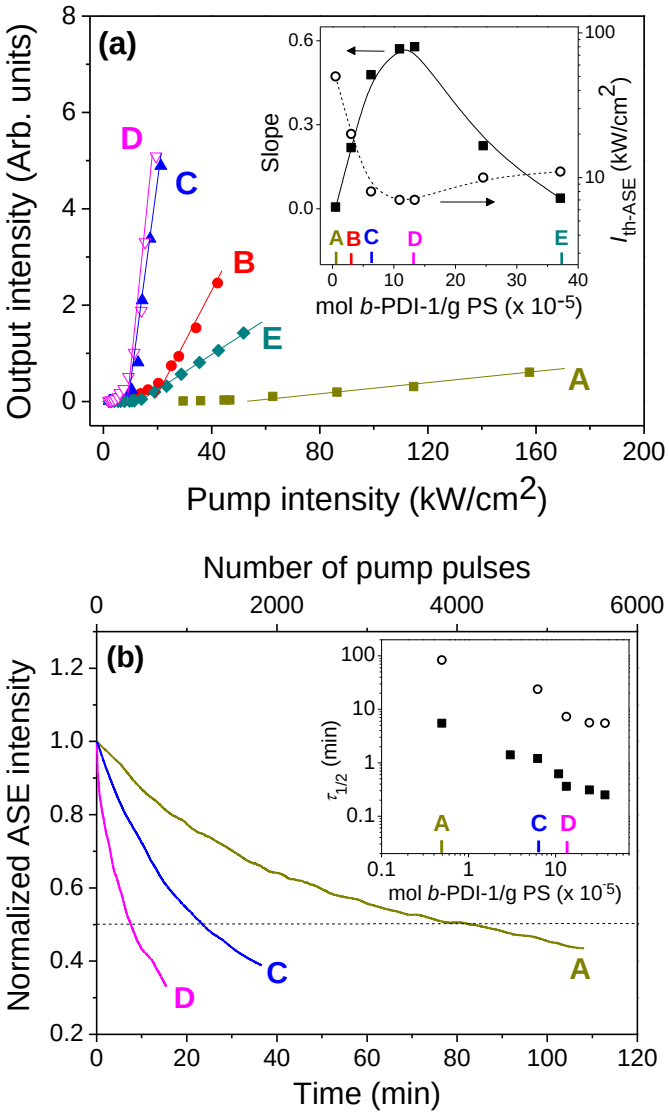
(a)
Output intensity (Arb. units)
Pump intensity (kW/cm2)
D
C
B
E
A
Slope
I th-ASE (kW/cm2)
A B C D E
mol b-PDI-1/g PS (x 10-5)
(b)
Number of pump pulses
Normalized ASE intensity
Time (min)
τ1/2 (min)
A C D
mol b-PDI-1/g PS (x 10-5)

Fig.2

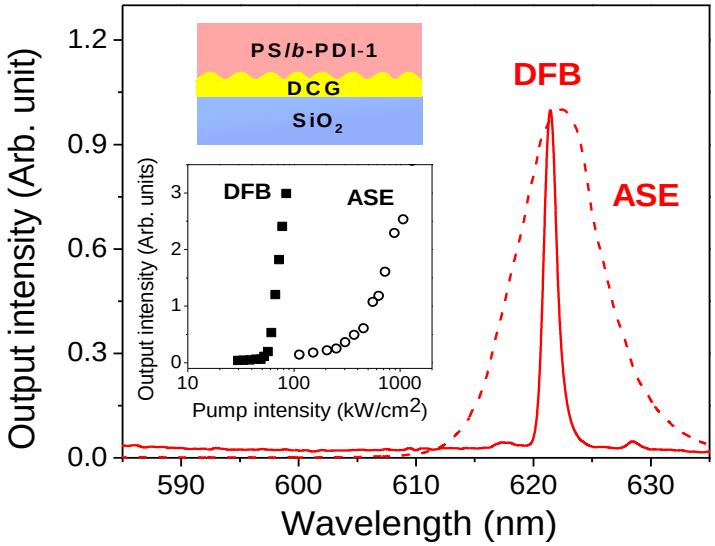
PS/b-PDI-1
DCG
SiO2
DFB
ASE
Output intensity (Arb. unit)
Wavelength (nm)
Output intensity (Arb. units)
Pump intensity (kW/cm2)

Fig.3

Figure Captions

Figure 1. (a) Chemical structures of *b*-PDI-1, *u*-PDI-2 and *b*-PDI-3; (b) PL intensity, integrated area below the spectrum divided by film thickness (main figure; circles) and PLQY as well as $\sigma_{em}(\lambda_{ASE})$ (inset; starts and diamonds, respectively) for PS films doped with different contents of *b*-PDI-1. PL data for *u*-PDI-2 and *b*-PDI-3 (main figure; squares and triangles), taken from refs. [6d] and [9a] respectively, are included for comparison purposes. Lines connecting points are guides to the eye; (c) Normalized PL and ASE spectra for various *b*-PDI-1-doped films (contents from left to right are: 0.5×10^{-5}, 11×10^{-5} and 37×10^{-5} mol of *b*-PDI-1 per gram of PS).

Figure 2. (a) Output intensity at the peak wavelength, as a function of pump intensity for films with different *b*-PDI-1 contents. Inset: ASE thresholds (circles) and slope efficiencies (squares), right and left axes respectively, versus *b*-PDI-1 content in the films. Capital letters are used to specify the concentrations of the films whose data are shown in the main figure; (b) Normalized ASE intensity versus irradiation time (bottom axis) and versus the number of pump pulses (10 ns, 10 Hz; top axis) for films with different *b*-PDI-1 contents, excited two times above their corresponding thresholds. Inset: Half-life versus *b*-PDI-1 content, when films are excited as in the main figure (circles) and at a fixed pump intensity of 2500 kW/cm^2 (squares).

Figure 3.- Laser spectrum (full line) of a DFB device (scheme shown in the top inset) based on a *b*-PDI-1 doped PS film (6×10^{-5} mol of *b*-PDI-1 per gram of PS) deposited over a grating recorded on dichromated gelatine (DCG). The ASE spectrum of the film in a region without grating is also included (dashed line); Bottom inset: Output intensity versus pump intensity for the DFB laser and for the film without grating.

Supporting Information

Click here to download Supporting Information: Revised Manuscript adom.201300301-Supporting Information.doc

Click here to download Production Data: Figure_1a.tif

Click here to download Production Data: Figure_1b.tif

Click here to download Production Data: Figure_1c.tif

Click here to download Production Data: Figure_2a.tif

Click here to download Production Data: Figure_2b.tif

Click here to download Production Data: Figure_3.tif

Click here to download Production Data: Graphical abstract.tif